

## Slab selective, regularized RF shimming

U. Katscher<sup>1</sup>, I. Graesslin<sup>2</sup>, K. Nehrke<sup>1</sup>, and P. Boernert<sup>1</sup>

<sup>1</sup>Philips Research Europe - Hamburg, Hamburg, Germany, <sup>2</sup>Philips Research Europe - Hamburg

**Introduction** RF shimming is a well-known technique, where amplitudes and phases of a transmit RF coil array are optimized to obtain a homogeneous  $B_1$  profile, i.e., to compensate wave propagation effects at main fields of 3T or above (see, e.g., [1]). Among other anatomies, legs are particularly prone to wave propagation effects due to their bi-cylindrical geometry, resulting in significant signal and contrast inhomogeneities. This study applies RF shimming using a whole-body, eight-channel Tx/Rx system at 3T [2,3] in an optimised way. A slab selective, separate but simultaneous excitation of two different regions was evaluated in the framework of frequency-encoded transmission (multi-frequency excitation "MULTIFEX") [4,5]. Furthermore, regularized RF shimming [6] was applied to avoid inhomogeneity compensation on the cost of high SAR.

**Theory** It is known from single channel excitation that multi-frequency RF pulses facilitate simultaneous multi-slab excitation [4]. For RF shimming, this concept offers the possibility to apply different  $B_1$  shim settings (amplitude and phase) to different parts of the body [5]. However, multi-frequency RF pulses suffer from increased SAR. A multi-transmit system might balance this disadvantage by driving different Tx elements at single, but different frequencies. For instance, the odd-numbered elements can be driven at frequency  $f_1$  encoding slab 1, the even numbered elements at frequency  $f_2$  encoding slab 2 [5]. In this case, the degrees of freedom per slab are reduced, however, also the occurring SAR.

$$\delta = (B_{1tot}(\mathbf{x}) - \bar{B}_{1tot})^2 + \lambda \sum_{n \leq N} A_n^2 / \bar{B}_{1tot}^2, \quad B_{1tot}(\mathbf{x}) = \sum_{n \leq N} A_n B_{1n}(\mathbf{x}) \quad (1)$$

Assuming that each slab is encoded by  $n = 1 \dots N$  transmit elements, the complex channel weights  $A_n = |A_n| \exp(i\varphi_n)$  are determined by minimizing the error function  $\delta$  (Eq. (1), see [6]) with  $B_{1n}$  the spatial sensitivity distribution of transmit channel  $n$  and  $\bar{B}_{1tot}$  the spatial average of  $B_{1tot}$ . The first term of  $\delta$  minimizes the  $B_1$  inhomogeneity. The second term of  $\delta$  minimizes the total forward RF power  $\sum_n A_n^2$  to avoid inhomogeneity compensation on the cost of high RF power. The freely adjustable regularization parameter  $\lambda$  describes the trade-off between the two terms. This approach indirectly helps to keep SAR low, which is a cheap alternative to the typically very extensive, exact SAR calculations. The obtained SAR reduction might be used to counterbalance the SAR increase caused by the introduction of multi-frequency RF pulses.

**Methods** A 3T MR system (Philips Achieva, Philips Medical System, Best, The Netherlands) equipped with an 8-element Tx/Rx body coil and the corresponding RF channels [2,3] was used. The transmit sensitivities  $B_{1n}$  of the thigh bones of 4 healthy volunteers were acquired using an inverted version of "Actual Flip angle Imaging" [7,8] (TR1/TR2/TE=40/200/3.5 ms,  $\alpha=70^\circ$ , voxel size  $8.7 \times 8.7 \times 10 \text{ mm}^3$ ). The following three RF shimming modes have been tested.

- (A) Simultaneously shimming of the legs with all 8 Tx elements.
  - (B) Separate shimming of the left and right leg using the 4 left and right Tx elements. This mimics two groups of Tx elements with different single frequency pulses, which encode the two sagittal slabs corresponding to the two legs.
  - (C) Separate shimming of the legs with all 8 Tx elements. This mimics dual frequency pulses, encoding the two sagittal slabs of the two legs.
- Furthermore, regularization was applied via Eq. (1) to minimize the total RF power. The obtained shim values were applied to an FDTD model [9] to confirm the inherent SAR reduction of the RF power regularization.

**Results** Fig. 1 compares the  $B_1$  maps of the standard quadrature mode (Q) with the above-described shimming modes (A)-(C) for an example volunteer. While standard RF shimming (A) removes a large part of the  $B_1$  inhomogeneities observed in quadrature mode, frequency encoded excitation shows a significant further reduction of the inhomogeneities. The difference between (B) and (C), i.e., using single/dual frequency pulses, seems to be negligible. Thus, for this volunteer, the single frequency mode (B) is preferable for the sake of lower SAR. Fig. 2 shows the corresponding results averaged over all 4 volunteers. Fig. 3 shows the influence of the regularization for shimming mode (B) for the example volunteer. Here, allowing a small  $B_{1tot}$  homogeneity degradation of, e.g., 2%, regularization is able to reduce the RF power by roughly a factor 3. Corresponding local SAR data from a FDTD model [9] confirm the correlation between RF power and local SAR (Fig. 3).

**Discussion / Conclusion** At 3T, large  $B_1$  inhomogeneities are visible in leg images, which can be compensated by the presented regularized slab-selective version of RF shimming. It is expected that also other applications, e.g., mammography, benefit from this localised RF shimming approach.

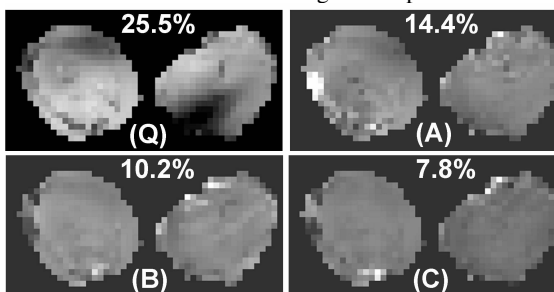


Fig. 1: Maps of  $B_{1tot}$  for standard quadrature excitation (Q) and the described shimming modes (A) standard RF shimming, (B) slab selective excitation with single and (C) dual frequency pulses. The numbers indicate the normalized root-mean-square error (NRMSE) of the different maps.

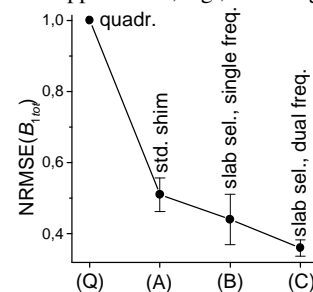


Fig. 2: Root-mean-square error of  $B_{1tot}$ , normalized to the quadrature excitation (Q), averaged over 4 volunteers. Slab selective excitation (B,C) can improve standard shimming results (A).

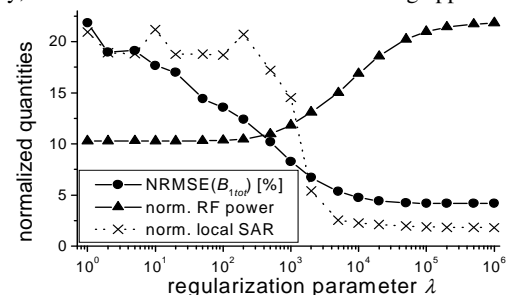


Fig. 3: Impact of regularization (exemplarily for shimming mode (B)). Allowing a certain  $B_{1tot}$  homogeneity degradation can lead to a reduction of the RF power. Corresponding local SAR data from a FDTD model [9] confirm the correlation between RF power and SAR reduction.

- References** [1] Ibrahim TS et al., MRI 18 (2000) 733 [2] Graesslin I et al., ISMRM 14 (2006) 129 [3] Vernickel P et al., MRM 58 (2007) 381 [4] Müller S, MRM 6 (1988) 364 [5] Katscher U et al., ISMRM 16 (2008) 1311 [6] Katscher U et al., Magn Reson Mater Phy 21 (2008) S63 [7] Yarnykh VL, MRM 57 (2007) 192 [8] Nehrke K et al., ISMRM 16 (2008) 353 [9] Graesslin I et al., ISMRM 14 (2006) 2041